Journal of Porphyrins and Phthalocyanines
J. Porphyrins Phthalocyanines 2017; **21**: 431–438
DOI: 10.1142/S1088424617500420

Published at http://www.worldscinet.com/jpp/

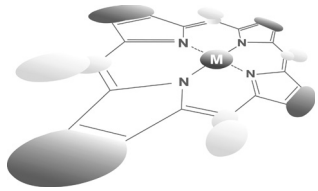

Photophysical studies of 2,6-dibrominated BODIPY dyes substituted with 4-benzyloxystyryl substituents

Bokolombe P. Ngoy, Nthabeleng Molupe, Jessica Harris, Gertrude Fomo, John Mack*◊ and Tebello Nyokong◊

Department of Chemistry, Rhodes University, Grahamstown 6140, South Africa

Dedicated to Professor Claudio Ercolani on the occasion of his 80th birthday.

Received 26 December, 2016
Accepted 14 April, 2017

ABSTRACT: A series of novel 2,6-dibrominated BODIPY dyes with styryl groups at the 3,5-positions has been prepared, and their photophysical properties have been analyzed to assess their potential utility for use as photosensitizers in photodynamic therapy and in bioimaging.

KEYWORDS: BODIPYs, singlet oxygen, Knoevenagel condensation, photophysics, fluorescence, TD-DFT calculations

INTRODUCTION

Photosensitization is the most important photoreaction in the context of singlet oxygen applications such as photodynamic therapy (PDT) [1], antimicrobial photodynamic therapy (PACT) [2, 3], and the photodegradation of organic pollutants [4]. The first singlet excited state of molecular oxygen lies at a relatively low energy and hence can be readily accessed through energy transfer from the triplet manifold of a photoexcited organic dye [5]. Singlet oxygen is cytotoxic and is hence useful for laser related biomedical applications. Photosensitizers such as porphyrins, phthalocyanines, naphthalocyanines, chlorins, bacteriochlorins, and texaphyrins [6–9] are among the most widely used dyes in PDT research. Structurally modified boron dipyrromethene (BODIPY) dyes [10–13] can also be used in this context. This family of dyes was first reported by Treibs and Kreuzer [14], and their derivatives have since been studied for a wide range of applications, such as use as laser dyes [15], as fluorescent switches [16] and as chemosensors [17]. Halogenation of BODIPY dyes enables a heavy atom effect which enhances the rate of intersystem crossing and hence the singlet oxygen quantum yield [18–20]. In recent years there has been a strong research focus on the synthesis and physicochemical studies of structurally modified BODIPY dyes that absorb the near infrared (NIR) region [18–22] which is most useful for biomedical applications. In this paper, we report the photophysical properties of BODIPY dyes functionalized with *p*-hydroxybenzaldehyde and *p*-benzyloxybenzaldehyde to form styryl groups at the 3,5-positions through Knoevenagel condensation reactions and we make use of TD-DFT calculations to analyze trends in their electronic structures and optical properties.

EXPERIMENTAL

Materials

2,4-Dimethylpyrrole, 4-bromobenzaldehyde, 4-formylbenzoic acid, 4-nitrobenzaldehyde, 4-hydroxybenzaldehyde, trifluoroacetic acid, *p*-chloranil, triethylamine, boron trifluoride diethyl etherate, *N*-bromosuccinimide, diphenylisobenzofuran, acetic acid, and piperidine were obtained from Sigma-Aldrich and were used without further purification unless otherwise noted. Dried solvents (supplied by Merck or Minema) were used for spectroscopic measurements, and 2,4-dimethylpyrrole was distilled before use.

◊SPP full member in good standing

*Dr. John Mack, email: j.mack@ru.ac.za.

Instrumentation

Ground state electronic absorption spectra were recorded on a Shimadzu UV-2550 spectrophotometer while fluorescence excitation and emission spectra were measured on a Varian Eclipse spectrofluorimeter. ^{1}H NMR spectra were recorded either on a Bruker 600 MHz or 300 MHz spectrometer in $CDCl_3$ or THF-d_8. Mass spectrometry was performed using a Bruker AutoFLEX III Smartbeam MALDI-TOF mass spectrometer and a dithranol matrix. Time-resolved fluorescence lifetime experiments were carried out in aerated solvents, by using a Picoquant GmbH time-correlated single photon counting (TCSPC) device containing a LDH-P-670 diode laser with a 44 ps pulse width and 20 MHz rate repetition. Exponential decay curves were analyzed by using Picoquant's Fluofit software package.

Photophysical measurements

The fluorescence quantum yields of BODIPY dyes **2a–2c** were obtained by using the comparative method with either Rhodamine 6G or zinc phthalocyanine (ZnPc) as the standard [23, 24]. The standard and sample solutions were excited at the same wavelength, and the solutions had identical optical densities. Singlet oxygen quantum yields (Φ_Δ) were determined in DMF, DMSO, EtOH, and THF solutions (in air without bubbling oxygen) using the relative method with Rose Bengal or ZnPc as the reference compound and 1,3-diphenylisobenzofuran (DPBF) as the singlet oxygen scavenger [25–29]. Solutions of the sample and reference photosensitizers containing DPBF were prepared in the dark and irradiated at a crossover wavelength. Photoirradiation for singlet oxygen determinations was carried out using a tunable laser system consisting of a Nd:YAG laser (355 nm, 135 mJ/4–6 ns) pumping an optical parametric oscillator (OPO, 30 mJ/4–6 ns) with a wavelength range of 420–2300 nm (NT-342B, Ekspla). All photophysical measurements were made in triplicate to ensure accuracy.

Synthesis

4-Benzyloxybenzaldehyde was prepared as a precursor for the Knoevenagel condensation reactions (Scheme1) and BODIPY dyes **2a–2c** were synthesized following three-step experimental procedure by synthesizing the BODIPY core followed by halogenations and Knoevenagel condensation to afford the desired target compounds (Schemes 2 and 3). The synthetic procedures used for the 8-(4-nitrophenyl) [30] and 8-(4-bromophenyl) [31] derivatives of 1,3,5,7-tetramethylBODIPY (**2a_H** and **2b_H**) and their 2,6-dibrominated analogs (**2a_Br** and **2b_Br**) [32, 33] have been reported previously, and the literature procedures were followed in each case. The absence of an ^{1}H NMR peak for 2,6-position protons was

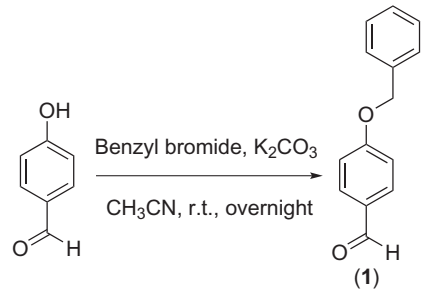

Scheme 1. Synthesis of 4-benzyloxybenzaldehyde (**1**).

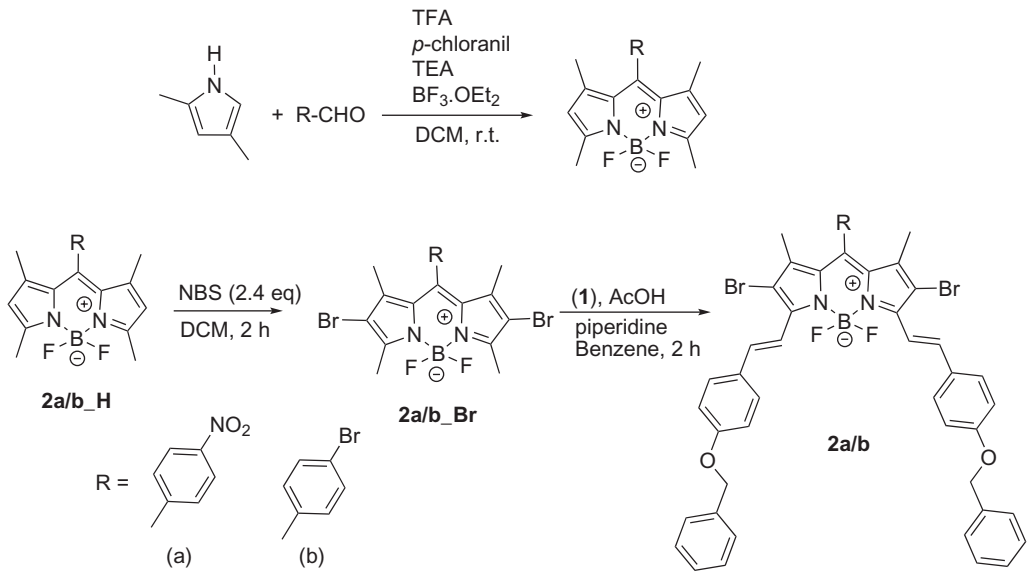

Scheme 2. Synthesis of BODIPY dyes **2a** and **2b** from two *meso*-aryl-substituted 1,3,5,7-tetramethyl BODIPYs (**2a/b_H**) and their 2,6-dibromo-substituted analogues (**2a/b_Br**).

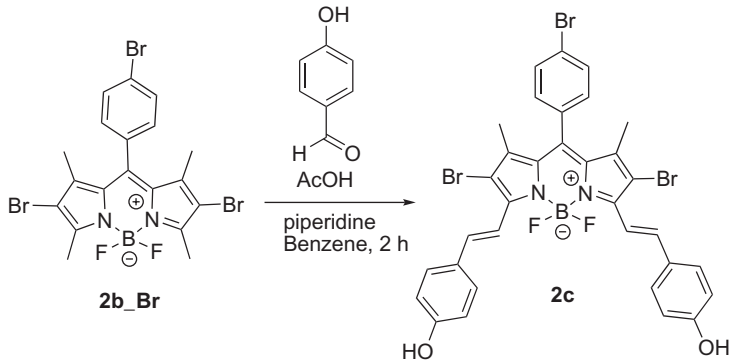

Scheme 3. Synthesis of BODIPY dye **2c** from 8-(4-bromophenyl)-2,6-dibromo-1,3,5,7-tetramethyl BODIPY (**2b_Br**).

checked to confirm the purity of **2a_Br** and **2b_Br**, which were obtained in 20% and 75% yield, respectively.

4-Benzyloxybenzaldehyde (1). A solution of 4-hydroxybenzaldehyde (4 g, 1 eq), benzyl bromide (5.6 g, 1 eq) and potassium carbonate (11.3 g, 2.5 eq) in 150 mL of acetonitrile was stirred at room temperature overnight. The solvent was evaporated on a rotary evaporator and the crude product was diluted with dichloromethane, washed with water (3 × 30 mL), dried over magnesium sulfate, concentrated to give the target compound **1** in 95% yield as a white solid after recrystallization from hot ethanol; IR (KBr, ν, cm^{-1}): 3056 (ArC-H), 2745–2829 (aliph), 1685 (C=O), 1574–1599 (C=C). ^{1}H NMR (300 MHz, THF-d8): δ 9.89 (s, 1H), 7.85 (*d*, *J* = 18.5 Hz, 2H), 7.49 (m, 2H), 7.42 (m, 3H), 7.15 (m, 2H), 5.21 (s, 2H) ppm. ^{13}C NMR (75 MHz, THF-d_8): δ = 189.43, 163.50, 136.70, 131.37, 130.60, 128.33, 127.83, 127.40, 114.90, 69.91 ppm.

BODIPY dyes (2a–2c). Glacial acetic acid (1 mL) and piperidine (1 mL) in benzene (50 mL) were added to solutions of 2,6-dibromo-1,7-methyl-4-nitrophenyl-BODIPY or 2,6-dibromo-1,7-methyl-4-bromophenyl-BODIPY (1 eq) and 4-benzyloxybenzaldehyde (2 eq). The mixture was refluxed for 2 h using a Dean-Stark apparatus to remove water formed during the reaction. The crude product was concentrated and then diluted with dichloromethane, washed with hydrochloric acid, sodium hydrogen carbonate, and brine. The target compounds **2a** and **2b** were obtained in very low and 20% yield, respectively, as dark green solids after silica column chromatography with petroleum ether-ethylacetate (4:1 v/v).

2a: ^{1}H NMR (600 MHz, $CDCl_3$): δ 8.18 (*d*, *J* = 16.6 Hz, 2H), 7.75 (*d*, *J* = 8.3 Hz, 2H), 7.68 (*d*, *J* = 8.6 Hz, 6H), 7.52 (*d*, *J* = 7.2 Hz, 4H), 7.48 (s, 4H), 7.41 (*d*, *J* = 7.3 Hz, 2H), 7.25 (s, 2H), 7.09 (s, 4H), 5.19 (s, 4H), 1.52 (s, 6H) ppm. MALDI-TOF (M+H): Calc. for $C_{47}H_{37}B_1Br_2F_2N_3O_4$: 916.1, found: 917.1.

2b: ^{1}H NMR (600 MHz, $CDCl_3$) δ 8.15 (s, 1H), 8.13 (s, 1H), 7.75–7.69 (m, 2H), 7.63 (dd, *J* = 10.3, 7.7 Hz, 6H), 7.48 (d, *J* = 7.4 Hz, 4H), 7.46–7.41 (m, 4H), 7.41–7.34 (m, 2H), 7.25–7.20 (m, 2H), 7.04 (d, *J* = 2.7 Hz, 4H), 5.16 (s, 4H), 1.48 (s, 6H) ppm. MALDI-TOF (M+H): Calc. for $C_{47}H_{37}B_1Br_3F_2N_2O_2$: 951.0, found: 951.9.

2,6-Dibromo-1,7-methyl-4-bromophenyl-BODIPY (0.1777 mmol) was dissolved in distilled benzene (50 ml). 3 eq of 4-hydroxybenzaldehyde was added and the solution stirred for 30 min. Under Dean-Stark reflux, the solution was heated gently in the presence of glacial acetic acid (0.4 ml) and piperidine (0.4 ml) for 45 min. The solution was cooled, then washed with water. The product was extracted using DCM, dried with anhydrous sodium sulfate and then filtered. The solvent was removed, and the product was isolated using silica column chromatography with 7:1 (v/v) petroleum ether/ethyl acetate as the eluent. **2c** was obtained as a dark green solid.

2c: Yield (147 mg, 74%): ^{1}H NMR (600 MHz, THF-d_8) δ 8.31 (d, *J* = 16.6 Hz, 2H), 7.96 (*d*, *J* = 8.2 Hz, 2H), 7.79 (*d*, *J* = 16.6 Hz, 2H), 7.68 (*d*, *J* = 8.5 Hz, 5H), 7.56 (*d*, *J* = 8.2 Hz, 2H), 7.00 (*d*, *J* = 8.5 Hz, 5H), 1.67 (s, 6H) ppm. MALDI-TOF (M+H): Calc. for $C_{33}H_{25}B_1Br_3F_2N_2O_2$: 770.9, found: 771.1.

Theoretical calculations

The density functional theory (DFT) method was used to carry out geometry optimizations for **2a–2c** by using the B3LYP functional of the Gaussian 09 program package [34] with 6-31G(d) basis sets. The same approach was used to calculate the electronic absorption properties by using the time-dependent DFT (TD-DFT) method with the CAM-B3LYP functional, which includes a long-range correction of the exchange potential and incorporates an increasing fraction of Hartree–Fock (HF) exchange as the interelectronic separation increases. The polarized continuum model was used to provide a tetrahydrofuran solvation environment for the geometry optimizations and the TD-DFT calculations.

RESULTS AND DISCUSSION

Synthesis

A series of novel halogenated and styrylated BODIPY dyes **2a–2c** were prepared using standard synthetic procedures so that their potential suitability for use in

biomedical applications could be assessed. As has been reported previously [21], halogenation and styrylation both result in a red shift of the main BODIPY spectral band, Fig. 1. The introduction of bromine atoms and nitro groups at the *para*-positions of the *meso*-aryl ring at the bridging 8-position of the BODIPY core provides scope for further structural modifications that would enable nanoparticle conjugation [35]. Nanoparticle conjugates are known to selectively accumulate in cancer tumors due to the enhanced permeability and retention effect. Studies on 2,6-diiodinated-3,5-styrylBODIPYs have suggested that the introduction of electron donating *meso*-aryl substituents in this context, such as aniline rings [35], could enhance the singlet oxygen quantum yield values [10, 11, 36, 37]. Benzyloxy groups were added to the styryl groups at the *para*-positions of the phenyl rings to form **2a** and **2b** so that their effect on the optical and photophysical properties could be explored.

Optical spectroscopy

Figure 2 contains normalized absorption spectra of **2a** and **2b** in a series of different solvents. The band maxima lie in the range of 668–684 nm, while emission bands are observed in the 680–720 nm region (Table 1). The band maxima of **2a–2c** (Table 1) lie in the therapeutic window (620–850 nm) making these chromophores potentially useful for photodynamic therapy and bioimaging. Trends in the optical properties and electronic structures of **2a–2c** (Figs 3–5) have been analyzed through a comparison of calculated TD-DFT spectra with those of model complexes of the analogous 1,3,5,7-tetramethyl-substituted BODIPY core with either H or Br atoms at the 2,6-positions corresponding to the precursors shown in Schemes 2 and 3. In each case, the transition to the S_1 state that gives rise to the main spectral band in the 600–700 nm region is predicted to be dominated by the HOMO → LUMO one-electron transition, Table 1, while the other intense bands that are observed in the 300–400 nm region (Fig. 1) can be assigned to transitions that are associated with MOs that are largely localized on the styryl groups (Fig. 5). As has been reported previously [21], when styryl groups replace the methyl group at the 3,5-positions of the BODIPY core, there is a significant decrease of the HOMO–LUMO gap (Fig. 4) and hence a large red-shift of the main BODIPY spectral band

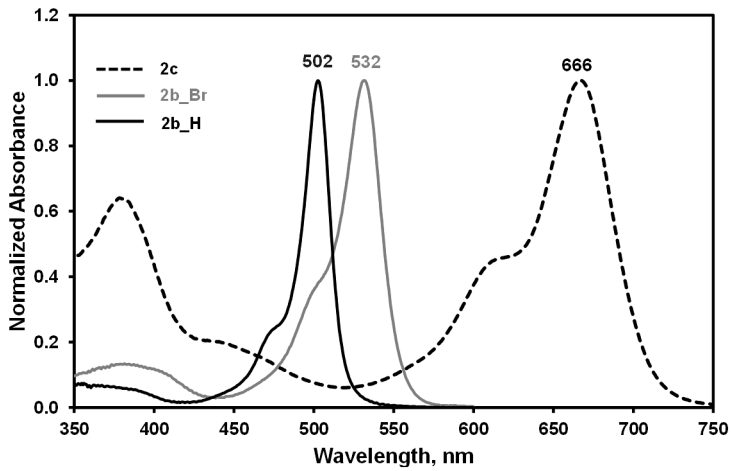

Fig. 1. Normalized absorption spectra of **2b_H**, **2b_Br**, and **2c** (Schemes 2 and 3) in dichloromethane.

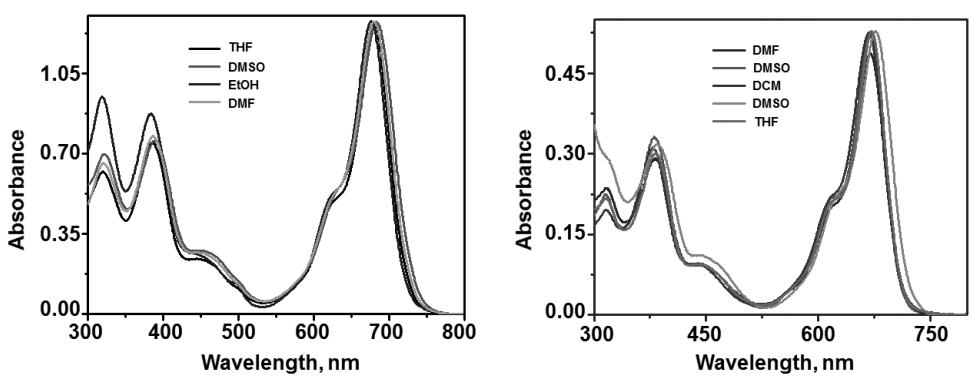

(a) (b)

Fig. 2. Solvent dependence of the absorption spectra of **2a** and **2b**.

Table 1. The main spectral bands in the TD-DFT spectra of the B3LYP optimized geometries of the two sets of tautomers of **2a–2c** at the CAM-B3LYP/6-31G(d) level of theory.

		Calc[a]		Exp[b]	Wave function[c] =
2a_H	($S_0 \rightarrow S_1$) 23.1	432	(0.63) 19.8	506	98% HOMO → LUMO; …
2a_Br	($S_0 \rightarrow S_1$) 22.3	449	(0.73) 18.8	532	98% HOMO → LUMO; …
2a	($S_0 \rightarrow S_1$) 16.6	601	(1.08) 14.7	680	95% HOMO → LUMO; …
2b_H	($S_0 \rightarrow S_1$) 23.3	430	(0.64) 19.9	502	98% HOMO → LUMO; …
2b_Br	($S_0 \rightarrow S_1$) 22.4	446	(0.73) 18.8	532	98% HOMO → LUMO; …
2b	($S_0 \rightarrow S_1$) 16.8	595	(1.07) 14.9	670	95% HOMO → LUMO; …
2c	($S_0 \rightarrow S_1$) 17.0	588	(1.06) 14.9	669	96% HOMO → LUMO; …

[a]Calculated band energies (10^3.cm^{-1}) and wavelengths (nm), with oscillator strengths in parentheses (f). [b]Observed energies (10^3.cm^{-1}) and wavelengths (nm) in THF or dichloromethane. [c]The wave functions based on the eigenvectors predicted by TD-DFT.

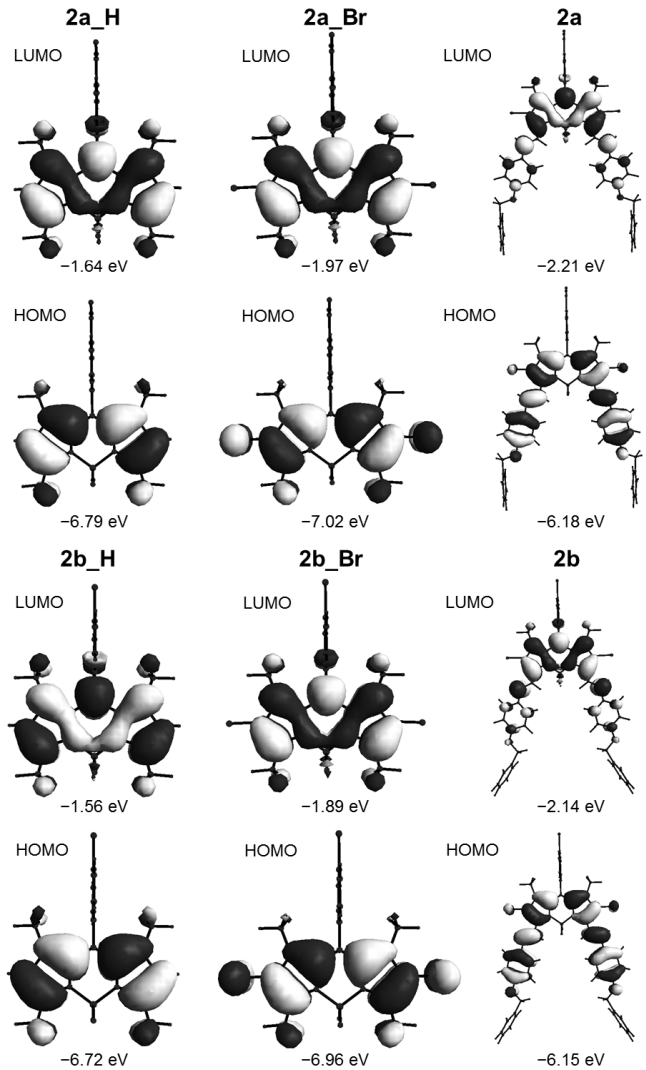

Fig. 3. MO energies and angular nodal patterns of the HOMO and LUMO of **2a** and **2b** and model complexes with no styryl moieties and either protons **(_H)** or bromine atoms **(_Br)** at the 2,6-positions.

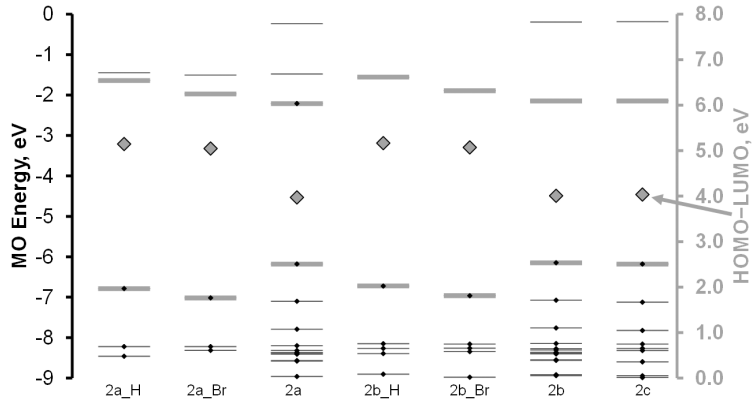

Fig. 4. MO energies of **2a–2c** and model complexes with methyl groups replacing the styryl moieties and either protons (_H) or bromine atoms (_Br) at the 2,6-positions. Occupied MOs are highlighted with small black diamonds. Gray lines are used to denote the HOMO and LUMO, while the HOMO–LUMO gap values are highlighted with gray diamonds and are plotted against a secondary axis.

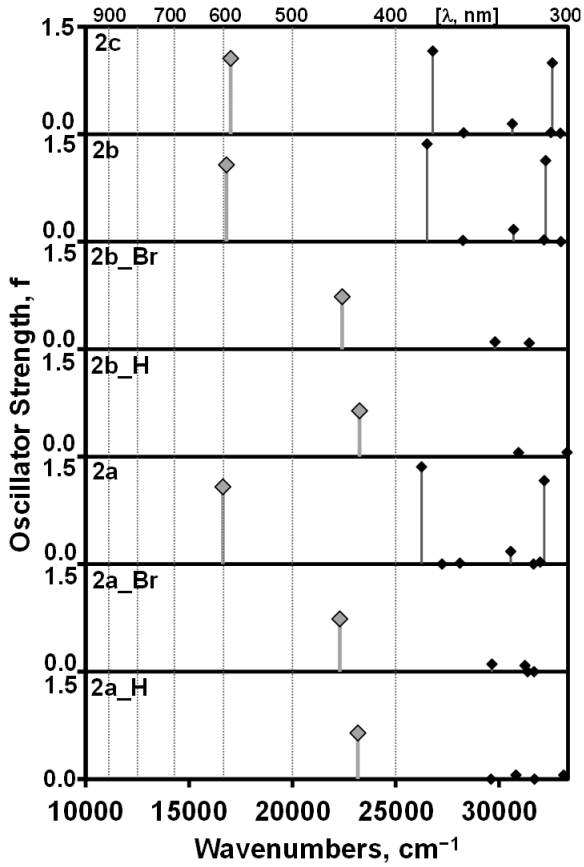

Fig. 5. Calculated TD-DFT spectra of **2a** and **2b** and model complexes with methyl groups replacing the styryl moieties and either protons (_H) or bromine atoms (_Br) at the 2,6-positions of the BODIPY core (Scheme 2). Gray diamonds are used to highlight the lowest energy transition that is assigned to the main spectral band (Table 2). Details of the calculations for this band are provided in Table 1.

(Fig. 5), since there are larger MO coefficients on the styryl group in the HOMO, due to the larger MO coefficients at the points of attachment on the BODIPY core (Fig. 3). The smaller red shift that is associated with bromination at the 2,6-positions (Fig. 5) can be readily explained by the mesomeric effect that is associated with the lone pair orbitals of the bromine atom, since there is a relative destabilization of the HOMO (Fig. 4), which has larger MO coefficients at these positions (Fig. 3). The attachment of a benzyloxy group at the *para*-position of the phenyl ring of the styryl group in the structure of **2b** has a similar effect on the energies of the frontier MOs to the hydroxyl group of **2c** (Fig. 4), so the spectra of **2b** and **2c** are predicted to be very similar, which matches what is observed experimentally (Table 2).

Photophysical properties

Table 2 provides the main photophysical parameters for **2a–2c**. The fluorescence lifetime values (τ_T) lie in the 2.0–3.5 ns range. In the absence of structural modifications, BODIPY dyes have unusually high fluorescence quantum yield values due to the rigid structure of the BODIPY core and very low triplet state quantum yield values [38]. Structural modifications can be used to form BODIPY dyes that have a combination of significant fluorescence and singlet oxygen quantum yield values. The combined utility for bioimaging and singlet oxygen generation along with the introduction of *meso*-aryl groups that can be further modified to enable nanoparticle conjugation makes the dyes potentially suitable for use in theranostics [39–43]. The introduction of bromine atoms to form the **2b_Br** 1,3,5,7-tetramethyl precursor results in a relatively high singlet oxygen quantum yield due to the heavy atom effect (Table 2). The

Table 2. Photophysical parameters for **2a–2c**, including the wavelengths of the band maxima in the absorption (λ_{max}) and emission (λ_{em}) spectra, the fluorescence lifetimes (τ_F) and the fluorescence (Φ_F) and singlet oxygen (Φ_Δ) quantum yield values.

	Solvent	λ_{max} [nm]	λ_{em} [nm]	τ_F [ns]	Φ_F	Φ_Δ
2a	EtOH	676	702	2.31	0.11	0.19
	DMSO	683	715	3.04	0.09	0.28
	DMF	680	711	3.33	0.07	0.24
	THF	680	703	3.42	0.13	0.34
2b	EtOH	668	—	3.04	—	0.23
	DMSO	677	715	2.90	0.12	0.26
	DMF	670	707	—	0.11	—
	THF	670	698	3.45	0.19	0.27
2b_Br	EtOH	532	543	3.81	0.30	0.65
	DMSO	530	546	—	0.18	0.82
2c	EtOH	666	706	2.72	0.09	0.16
	DMSO	680	716	—	0.21	0.10
	DMF	676	712	—	0.26	0.10
	THF	674	701	3.15	0.21	0.11

values for **2a–2c** are significantly lower, however, since the introduction of the styryl groups can be expected to result in S_1 states with significant intramolecular charge transfer character, since there are greater MO coefficients on the styryls in the HOMO than in the LUMO (Fig. 3). This is known to result in enhanced rates of non-radiative decay, especially when polar solvents are used [44, 45]. A comparison of the singlet oxygen quantum yield values for **2b** and **2c** demonstrates that the incorporation of the benzyloxy groups slightly enhances the Φ_Δ, possibly due to a change in the efficiency of energy transfer from the T_1 state of the BODIPY dye, while in contrast, the fluorescence quantum yield values are somewhat lower possibly due to the enhanced conformational flexibility (Table 2). Since there is no red shift of the absorption band towards the center of the therapeutic window, there is no obvious advantage derived from incorporating these groups beyond the possibility of enhanced solubility in the context of aqueous solvents, if for example the *meso*-aryl ring of **2a** were further modified to introduce a quaternized nitrogen atom, as π–π stacking involving the planar styryl groups would be hindered.

CONCLUSIONS

A series of novel brominated and styrylated BODIPY dyes have been prepared. The introduction of bromine atoms at the 2,6-positions results in dyes with significant fluorescence and singlet oxygen quantum yield values making them potentially suitable for use in theranostics. The presence of benzyloxy moieties on the styryl groups results in a relatively low singlet oxygen quantum yield value and has almost no effect on the wavelength of the main BODIPY spectral band when a comparison is made with an analgous dye that contains hydroxyl groups, but enhanced solubility is anticipated in polar solvents, since aggregation due to π–π stacking of the planar styryl groups is hindered. Studies are underway to identify structural modifications that further enhance the photophysical properties of styrylated BODIPY dyes in a manner that makes them suitable for use in biomedical applications.

Acknowledgements

Financial support was provided by an NRF of South Africa CSUR grant (uid: 93627) to JM and a Pearson Young Memorial Scholarship to NM. Theoretical calculations were carried out at the Center for High Performance Computing in Cape Town and photophysical measurements were made possible by the were made possible by the Laser Rental Pool Programme of the Council for Scientific and Industrial Research (CSIR) of South Africa.

REFERENCES

1. Jesionek A and von Tappeiner H. *Arch. Klin. Med.* 1905; **82**: 223–227.
2. Hamblin MR and Hasan T. *Photochem. Photobiol. Sci.* 2004; **3**: 436–450.
3. Wainwright M. *Photochem. Photobiol. Sci*. 2004; **3**: 406–411.
4. Kim H, Kim W, Mackeyev Y, Lee G-S, Kim H-J, Tachikawa T, Hong S, Lee S, Kim J, Wilson LJ, Majima T, Alvarez PJJ, Choi W and Lee J. *Environ. Sci. Technol.* 2012; **46**: 9606−9613.
5. Khan AU and Kasha M. *J. Am. Chem. Soc.* 1970; **92**: 3293−3300.
6. Ali H and van Lier JE. *Chem. Rev.* 1999; **99**: 2379−2450.
7. Drzewiecka A, Urbanska K, Matuszak Z, Pineiro M, Arnout LG, Habdas J, Ratuszna A and Stochel G. *Acta Biochim. Pol.* 2001; **48**: 277−282.
8. Nyman ES and Hynnien PH, *J. Photochem. Photobiol. B* 2004; **73**: 1−28.
9. Detty MR, Gibson SL and Wagner SJ. *J. Med. Chem.* 2004; **47**: 3897−3915.
10. Atilgan S, Ekmekci Z, Dogan AL, Guc D and Akkaya EU. *Chem. Commun.* 2006; **42:** 4398–4400.
11. He H, Lo P-C, Yeung S-L, Fong W-P and Ng DKP. *J. Med. Chem.* 2011; **54**: 3097−3102.

12. Kamkaew A, Lim SH, Lee HB, Kiev LV, Chung LY and Burgess K. *Chem. Soc. Rev.* 2013; **42**: 77–88.
13. Lim SH, Thivierge C, Nowak-Sliwinska P, Han J, van den Bergh H, Wagnieres G, Burgess K and Lee HB. *J. Med. Chem.* 2010; **53**: 2865–2874.
14. Treibs A and Kreuzer FH. *Justus Liebigs Ann. Chem.* 1968; **718**: 208–223.
15. Arbeloa TL, Arbeloa FL, Arbeloa IL, Garcia-Moreno I, Costela A, Sastre R and Amat-Guerri F. *Chem. Phys. Lett.* 1999; **299**: 315–321.
16. Trieflinger C, Rurack K and Daub J. *Angew. Chem. Int. Ed.* 2005; **44**: 2288–2291.
17. Gabe Y, Ueno T, Urano Y, Kojima H and Nagano T. *Anal. Biochem.* 2006; **386**: 621–626.
18. Byrne AT, O'Connor AE, Hall M, Murtagh J, O'Neill K, Curran KM, Mongrain K, Rousseau JA, Lecomte R, McGee S, Callanan JJ, O'Shea DF and Gallagher WM. *Br. J. Cancer* 2009; **2a**: 1565–1573.
19. Yogo T, Urano Y, Ishitsuka Y, Maniwa F and Nagano T. *J. Am. Chem. Soc.* 2005; **127**: 12162–12163.
20. IUPAC Compendium of Chemical Terminology, 2nd Edn., McNaught AD and Wilkinson A (Eds.) Blackwell Scientific Publications: Oxford, UK, 1997; Vol. 68, p. 2245.
21. Lu H, Mack J, Yang Y and Shen Z. *Chem. Soc. Rev.* 2014; **43**: 4778–4823.
22. Killoran J, Allen L, Gallagher JF, Gallagher WM and O'Shea DF. *Chem. Commun.* 2002; **17**: 1862–1863.
23. Ogunsipe A, Maree D and Nyokong T. *J. Mol. Struct.* 2003; **650**: 131–140.
24. Sibata MN, Tedesco AC and Marchetti JM, *Eur. J. Pharm. Sci.* 2004; **23**: 131–138.
25. Ogbodu RO, Antunes E and Nyokong T. *Polyhedron* 2013; **60**: 59–67.
26. Carloni P, Damiani E, Greci L, Stipa P, Tanfani F, Tartaglini E and Wozniak M. *Res. Chem. Int.* 1993; **19**: 395–405.
27. Maree SE and Nyokong T. *J. Porphyrins Phthalocyanines* 2001; **5**: 782–792.
28. Redmond RW and Gamlin JN. *J. Photochem. Photobiol.* 1999; **70**: 391–475.
29. Jiang X. *Chem. Commun.* 2010; **46**: 3188–3190.
30. Jameson LP and Dzyuba SV, Beilstein. *J. Org. Chem.* 2013; **9**: 786–790.
31. Wang L, Fang G and Cao D. *J. Fluoresc.* 2014; **24**: 1757–1766.
32. Cihaner A and Algi F. *React. Funct. Polym.* 2009; **69**: 62–67.
33. Algi MP, Tirkes S, Ertan S, Ergun EGC and Cihaner A, *Algi. Electrochim. Acta* 2013; **109**: 766–774.
34. Gaussian 09, Revision E.01, Frisch MJ, Trucks GW, Schlegel HB, Scuseria GE, Robb MA, Cheeseman JR, Scalmani G, Barone V, Mennucci B, Petersson GA, Nakatsuji H, Caricato M, Li X, Hratchian HP, Izmaylov AF, Bloino J, Zheng G, Sonnenberg JL, Hada M, Ehara M, Toyota K, Fukuda R, Hasegawa J, Ishida M, Nakajima T, Honda Y, Kitao O, Nakai H, Vreven T, Montgomery Jr. JA, Peralta JE, Ogliaro F, Bearpark M, Heyd JJ, Brothers E, Kudin KN, Staroverov VN, Kobayashi R, Normand J, Raghavachari K, Rendell A, Burant JC, Iyengar SS, Tomasi J, Cossi M, Rega N, Millam JM, Klene M, Knox JE, Cross JB, Bakken V, Adamo C, Jaramillo J, Gomperts R, Stratmann RE, Yazyev O, Austin AJ, Cammi R, Pomelli C, Ochterski JW, Martin RL, Morokuma K, Zakrzewski VG, Voth GA, Salvador P, Dannenberg JJ, Dapprich S, Daniels AD, Farkas Ö, Foresman JB, Ortiz JV, Cioslowski J and Fox DJ. Gaussian, Inc., Wallingford CT, 2009.
35. Kubheka G, Uddin I, Amuhaya E, Mack J and Nyokong T. *J. Porphyrins Phthalocyanines* 2016; **20**: 1016–1024.
36. He H, Lo P-C, Yeung S-L, Fong W-P and Ng DKP. *Chem. Commun.* 2011; **47**: 4748–4750.
37. Gibbs JH, Robbins LT, Zhou Z, Bobadova-Parvanova P, Cottam M, McCandless GT, Fronczek FR and Vicente MGH. *Bioorg. Med. Chem.* 2013; **21**: 5770–5781.
38. Loudet A and Burgess K. *Chem. Rev.* 2007; **107**: 4891–4932.
39. Gibbs JH, Zhou Z, Kessel D, Fronczek FR, Pakhomova S and Vicente MGH. *J. Photochem. Photobiol. B* 2015; **145**: 35–47.
40. Cantu R, Gobeze HB, Nesterov VN, Das SK and D'Souza F. *Chem. Asian J.* 2015; **10**: 1335–1343.
41. Yang Y, Guo Q, Chen H, Zhuo Z, Guo Z and Shen Z. *Chem. Commun.* 2013; **49**: 3940–3942.
42. Tasan S, Zava S, Bertrand B, Bernhard C, Goze C, Picquet M, Le Gendre P, Harvey P, Denat F, Casini A and Bodio E. *Dalton Trans.* 2013; **42**: 6102–6109.
43. Lee MH, Sessler JL and Kim JS. *Acc. Chem. Res.* 2015; **48**: 2935–2946.
44. Rurack K, Kollmannsberger M and Daub J. *Angew. Chem. Int. Ed.* 2001; **40**: 385–387.
45. Gai L, Mack J, Lu H, Yamada H, Kuzuhara D, Lai G, Li Z and Shen Z. *Chem. Eur. J.* 2014; **20**: 1091–1102.